SIMULTANEOUS SENSOR AND PROCESS FAULT DIAGNOSTICS
FOR PROPELLANT FEED SYSTEM

J. Cao[+], C. Kwan[&], R. Xu[&], and F. Figueroa*

[+]*ACI Worldwide,* [&]*Intelligent Automation, Inc.,*
**NASA Stennis Space Center*

Abstract: The main objective of this research is to extract fault features from sensor faults and process faults by using advanced fault detection and isolation (FDI) algorithms. A tank system that has some common characteristics to a NASA testbed at Stennis Space Center was used to verify our proposed algorithms. First, a generic tank system was modeled. Second, a mathematical model suitable for FDI has been derived for the tank system. Third, a new and general FDI procedure has been designed to distinguish process faults and sensor faults. Extensive simulations clearly demonstrated the advantages of the new design.

Keywords: Fault Diagnosis, Fault Detection, Fault Isolation, Simulation.

1. TANK MODEL DEVELOPMENT

The purpose of modeling a tank system is to provide the simulated data of the process, including data from the normal situation and also data from some typical fault situations. All the generated data sets will be used for evaluating the performance of the various FDI algorithms.

Based on input from NASA, the tank system includes a liquid oxygen (LOX) tank, vertical pipe line, nitrogen tank, horizontal pipe line, and two valves, one is a three-way valve for liquid; the other is for gas. We assume the complete gaseous state after the second valve and the complete liquid state before the second valve. This assumption may not be realistic. However, making everything liquid is straightforward. The full picture of the diagram is shown in Fig.1.

Ullage and Nitrogen Tank
The gas in the ullage of the tank is assumed to follow the ideal gas law

$$p_u = \frac{M_{O_2} R T_u}{V_u}, \qquad p_n = \frac{M_{Nr} R T_n}{V_n}, \tag{1}$$

$$\frac{dM_{Nr}}{dt} = \rho_{Nr} v_{Nr}. \tag{2}$$

where R is gas constant, M_{O2} and M_{Nr} are respective gas oxygen and gas nitrogen holdup in mole, ρ_{Nr} is the nitrogen density.

Dynamics of Liquid Level
The dynamic process of the liquid level in the tank (Marlin, 1995) can be described as

$$\frac{dL}{dt} = -K_F L^{0.5}. \tag{3}$$

Here K_F is the level dynamic constant and S_F is the inlet area of the tank. Correspondingly, the volume of the ullage is described as

$$\frac{dV_u}{dt} = V_{u0} - S_F(L)\frac{dL}{dt} \tag{4}$$

where V_{u0} is the initial volume of the ullage space.

Fluid Mechanism
We utilize the mechanical energy equation of steady incompressible flow (Gerhart, 1992) to describe the dynamics of the liquid fluid

$$\frac{p_1}{\rho} + \frac{v_1^2}{2} + gz_1 = \frac{p_2}{\rho} + \frac{v_2^2}{2} + gz_2. \tag{5}$$

Here two arbitrary locations, namely 1 and 2, along the pipe are considered. The p_1 and p_2, v_1 and v_2, z_1 and z_2, are the respective pressure, flowrate, and height at these points.

Mass Balance
This law is based on the fact that the mass of the total input material should be equal to the mass of the total output material of a system no matter what has happened inside the system. The specific balance equations are

$$\rho_{liquid} v_3 S_P = \rho_{gas} v_2 S_P = \rho_{gas} v_1 S_P \tag{6}$$

where ρ_{liquid} and ρ_{gas} are the density of the liquid fluid and the gas fluid, v_{i} are the flow rate, and S_F and S_P

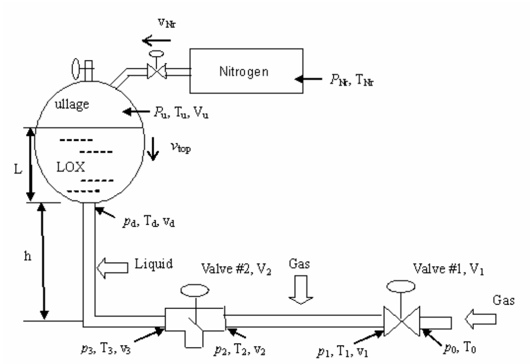

Fig.1 External tank schematics

are the inlet areas of the tank and the pipe line, respectively. Note that the flow rate v_1 is equal to v_2 based on the law.

Simplified Temperature Dynamics

In the ullage, the temperature dynamics can be described as

$$\frac{dT_u}{dt} = \frac{kv_{Nr}(T_{Nr} - T_u)}{M} \tag{7}$$

where k is a heat transfer constant, M is the total holdup (gas oxygen and gas nitrogen) in the ullage space.

We consider the general energy equation for steady compressible flow (Gerhart, 1992) along the streamline

$$T_2 = T_1 + \frac{v_1^2 - v_2^2}{2C_p}. \tag{8}$$

Here two arbitrary locations, namely 1 and 2, along the stream of the gas fluid are considered. C_p is the heat transfer constant, the T_1 and T_2, v_1 and v_2, are the respective temperature and flow rate.

Valve Model

We apply the general valve model (Marlin, 1995) to our process

$$F = C_v V \sqrt{\frac{\Delta p}{\rho}} \tag{9}$$

where C_v is the valve coefficient, V is the valve opening position, F is the mass flow rate, Δp is the pressure difference, and ρ is the density of the fluid.

Table 1: Summary of the tank system parameters

System parameters are chosen as: a = 1.360, b = 0.03803, R_0 = 8314, r_{tank} = 1.2m, and $S_F = 0.1464\text{m}^2$, C_p = 1kcal/(K, mol), C_1 = 1, C_2 = 2, K_F = 0.35, k = 1
The initial values of some process variables are: T_u = 50K, T_0 = 215K, $p_0 = 1\times10^5$Pa, L_0 = 2.0m, $p_{u0} = 1.51\times10^5$Pa, v_{top0} = 0 m/sec, p_{Nr} = 8.92e7Pa(13,000 PSI).

The whole simulation has been realized by MATLAB. Simulated process noise and measurement noise have been added to some variables. In Fig.2, the simulated dynamic behaviors in measurement variables and state variables have been shown. It can be seen that the system behavior is nonlinear, especially during the initial phase and around sample 500.

2. DERIVATION OF A PRIMARY RESIDUAL MODEL FOR FDI

As can be seen from the previous section, the tank system is a nonlinear dynamic system. To deal with the nonlinearity in the tank system, we used a piecewise linearization approach. Although this approach is simple, the accuracy of our model is actually quite well as we will see shortly.

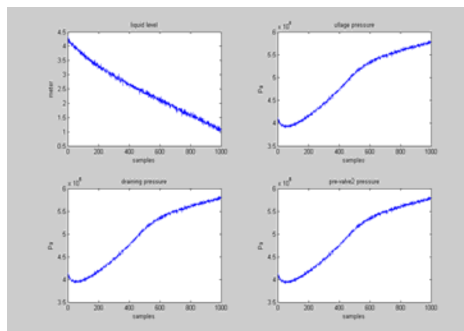

(a) Measurement Variables

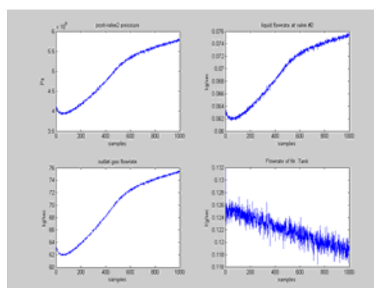

(b) Measurement variables

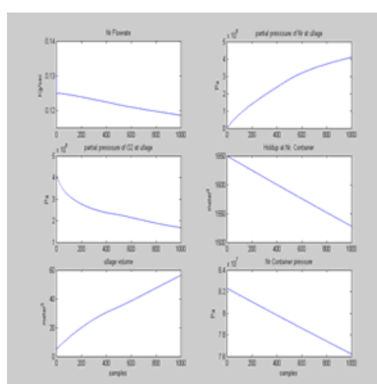

(c) State variables

Fig.2 Simulated process dynamics of a tank in normal situation

Let $\mathbf{x}$ be the vector of process variables containing inputs and outputs and $\mathbf{B}$ the system parameter matrix. Suppose $\mathbf{X}$ is a collection of vectors of $\mathbf{x}$. Then $\mathbf{X}$ can be decomposed by using *Singular Value Decomposition* (SVD)

$$\mathbf{X} = \mathbf{P}\,\Sigma\mathbf{Q}^{\mathrm{T}} \tag{10}$$

or by eigenstructure decomposition of the covariance matrix $\boldsymbol{R}$ of $\boldsymbol{x}$

$$\mathbf{R} = \mathbf{Q}\Lambda\mathbf{Q}^{\mathbf{T}}. \tag{11}$$

where $\mathbf{R} = \dfrac{1}{N}\sum_{i=1}^{N} x_i x_i^T$. The eigenvector matrix $\mathbf{Q}$, which can be decomposed into $[\mathbf{Q}_1 \;\; \mathbf{Q}_2]$, consists of the *representation subspace* $\mathbf{Q}_1$ and the *residual subspace* $\mathbf{Q}_2$. The number of the columns in the $\mathbf{Q}_2$, which is a column-normalized matrix, is equal to the number of the linear relations (same as the number of outputs). The subspace theory indicates that $\mathbf{Q}_2$ is in the same subspace with $\mathbf{B}^{\mathrm{T}}$. Thus, the matrix $\mathbf{Q}_2$ can be considered as an estimate of parameter matrix $\mathbf{B}^{\mathrm{T}}$ in real systems. That is,

$$\mathbf{B} = \mathbf{Q}_2^T. \tag{12}$$

It can be seen that (12) is directly derived from the sensor data. We will use this model to design the FDI algorithms.

Here we use Q^2 testing to validate the residual model. We first used a single model for the whole process. The result of Q^2 testing is shown in Fig. 3. The Q^2 value is 0.0046. Obviously, this linearized approximation is not satisfactory, especially at the beginning, 400$^{\text{th}}$, and 1000$^{\text{th}}$ sample regions. We then considered a piecewise linearization approach. The results of Q^2 testing for one model and two-model approaches are both shown in Fig. 4 (the solid line is from Fig. 3 and the dotted line is the Q^2 testing result by using two linearized models. Fig. 4 indicates that the piece-wise modeling yields much smaller error than the original approach.

Therefore, we can utilize the piece-wise modeling approach to model the nonlinear tank system. That is, we use the first batch data from 1 to 400 to build the first linear model and use the second batch data from 401 to 1000 to create the second linear model. Based on these two linear models, we can approximate the nonlinear system very well even though both the linear models are static in nature.

3. SIMULTANEOUS FAULT FEATURE EXTRACTION FOR PROCESS AND SENSOR FAULTS IN THE PRESENCE OF DISTURBANCE

3.1 Problem Formulation Motivation

We consider the effect of *process disturbances*, which behaves like unknown inputs and is shown below

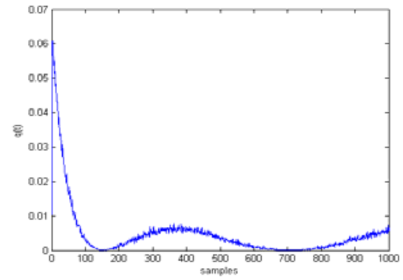

Fig. 3 Q^2 testing for a single model

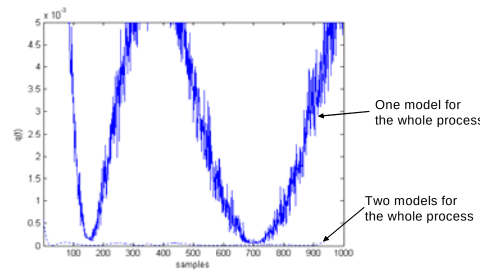

Fig. 4 Comparison of Q^2 testing results for the single model and the piecewise two-model approaches

$$\mathbf{y}(t) = \mathbf{A}\mathbf{u}(t) + \mathbf{F}\mathbf{p}(t) + \mathbf{K}\mathbf{d}(t) + \varepsilon(t) \tag{13}$$

where $\mathbf{K}$ is the disturbance transformation matrix, $\mathbf{d}(t) = [d_1(t) \;\; d_2(t) \;\ldots\; d_h(t)]^{\mathrm{T}}$. We assume there are h types of disturbance.

Combining the sensor and process faults in the presence of disturbances, (13) can be re-written as

$$\mathbf{B}\,\mathbf{x}(t) = \mathbf{B}\Delta\mathbf{x}(t) + \mathbf{F}\mathbf{p}(t) + \mathbf{K}\mathbf{d}(t) + \varepsilon(t) \tag{14}$$

where $\mathbf{x}(t)$ represents the observations. Note that we assume the transformation matrices, $\mathbf{F}$ and $\mathbf{K}$, are known. But $\mathbf{p}(t)$ and $\mathbf{d}(t)$ are unknown.

Equation (14) can be written in more compact form as

$$\mathbf{e}(t) = \mathbf{B}\mathbf{x}(t) = \mathbf{C}\mathbf{s}(t) + \mathbf{K}\mathbf{d}(t) + \varepsilon(t) \tag{15}$$

where $\mathbf{C} = [\mathbf{B} \;\; \mathbf{F}]$, $\mathbf{s}(t) = [\Delta\mathbf{x}(t)^{\mathrm{T}} \;\; \mathbf{p}(t)^{\mathrm{T}}]^{\mathrm{T}}$, $\mathbf{e}(t)$ is the set of *primary residuals* which are computed from the observations but depend only on the faults and noise.

For fault isolation, the structured or enhanced residuals are then obtained by a transformation $\mathbf{W}$ to yield

$$\boldsymbol{r}(t) = \mathbf{W}\mathbf{e}(t) = \mathbf{W}\mathbf{C}\,\mathbf{s}(t) + \mathbf{W}\mathbf{K}\mathbf{d}(t) + \mathbf{W}\varepsilon(t) \tag{16}$$

Hence, we need to derive a more powerful FDI scheme, which can:

(1) Decouple disturbance from faults;
(2) Detect two types of faults, sensor fault and process fault, in one framework;
(3) Diagnose simultaneous faults from different fault types;
(4) Identify fault sizes in the various fault situations.

In the next section, we present an approach that can achieve all of the above requirements. Here we present a general approach to extract fault features for both sensor and process faults in the presence of process disturbances.

3.2 Structured Residual Design

Disturbance Decoupling

The disturbance behaves like an unknown input. From Eq. (14), we can clearly see that it affects the primary residual. Since our focus is to detect and isolate sensor and process faults, we have to decouple its effect on the residual by designing **W** such that

$$\mathbf{WK} = 0 \tag{17}$$

This means the effects of disturbances will be annihilated. The price we pay for this decoupling is that we will lose some degrees of freedom in maximizing the amplitude of structured residuals. Moreover, we may lose some freedoms in simultaneous fault isolations. However, disturbances will affect the fault detection and isolation performance if we do not decouple them. Thus, we have to pay the price to cancel the disturbance effects.

Fault Isolation

For fault isolation, the goal is to develop a structured residual scheme. That is, the i^{th} row of **W**, $\mathbf{w}_i^T$ is designed so that the zeros assigned for the i^{th} row of the structure matrix can be implemented. This requires that

$$\mathbf{w}_i^T \mathbf{C}^{i\#} = \mathbf{0} \tag{18}$$

where $\mathbf{C}^{i\#}$ contains those columns of the matrix **C**, which is [**B** **F**], which belong to the faults assigned for zero response in the *i*th residual structure. On the other hand, the other part of matrix **C**, $\mathbf{C}^i$, should satisfy

$$\mathbf{w}_i^T \mathbf{C}^{i} = \mathbf{v}_i^T \tag{19}$$

Here each element of the vector $\mathbf{v}_i$ must be nonzero. Obviously, in order to design the structured residuals that are able to isolate faults from sensor faults and process faults, and to be free from the effect of disturbances, Eqs. (17)-(19) should be satisfied. Finally, we mentioned there are ways to optimize $\mathbf{w}_i^T$ by using a max-min procedure (Xu and Kwan 2003) so that the isolation residuals will be robust to measurement noise.

Simultaneous Fault Isolation

When more than one fault is present in the system simultaneously, the effect of these faults on the residuals will be added up. In other words, the combination of the effects is algebraic. It is possible to construct residual structures with multiple fault isolation. Table 2 shows an incidence matrix that can perform multiple fault isolation. There are 4 faults and 4 residuals. It can be seen that, for example, fault code [1 0 0 0] corresponds to fault x_1 and [1 1 0 0] corresponds to simultaneous faults in x_1 and x_2.

Table 2 Fault codes for multiple faults isolation

	x_1	x_2	x_3	x_4	x_1x_2	x_1x_3	x_1x_4	x_2x_3	x_2x_4	x_3x_4
r_1	1	0	0	0	1	1	1	0	0	0
r_2	0	1	0	0	1	0	0	1	1	0
r_3	0	0	1	0	0	1	0	1	0	1
r_4	0	0	0	1	0	0	1	0	1	1

We will use incidence matrices that are similar to the above one in our design.

Fault Identification (Fault size estimation)

After fault isolation, it is also important to determine the fault magnitude, which will tell us the seriousness of the fault. Here we present an approach to estimate the fault size. For simplicity, we do not consider the disturbance term in the next few paragraphs. In the presence of disturbances, we may use the decoupling technique to decouple the disturbances.

From Eq. (15), we have

$$\mathbf{e}(t) = \mathbf{Bx}(t) = \mathbf{Cs}(t) + \varepsilon(t) \tag{20}$$

where $\mathbf{C} = [\mathbf{B}\ \ \mathbf{F}]$, $\mathbf{s}(t) = [\Delta\mathbf{x}(t)^T\ \ \mathbf{p}(t)^T]^T$, $\mathbf{e}(t)$ is the primary residual. If the i^{th} fault has been detected and isolated, we only need to pay attention to i^{th} column of the matrix **C**. That is,

$$\mathbf{e}(t) = \mathbf{c}_i\, s_i\,(t) + \varepsilon(t)$$

where $s_i\,(t)$ could be either sensor faults or process faults. From the fault isolation step, we would have known what faults have occurred. There are two approaches to perform the estimation. For a single fault, one may directly compute its size as

$$\hat{s}_i(t) = mean(\mathbf{e}(t)./\mathbf{c}_i)$$

Note that "./ " means dot division. The estimated fault size has been smoothed by taking the mean value. As for the simultaneous faults, the Least Square (LS) estimation method should be used, which is given by

$$\hat{\mathbf{s}}_i(t) = (\mathbf{c}_i^T \mathbf{c}_i)^{-1} \mathbf{c}_i^T \mathbf{e}(t)$$

3.3 Simulation Experiments

Here we employ the tank model to demonstrate the above approach. We use 6 variables to illustrate the design procedures and performance. They are: L, P_u, P_2, v_1, P_{Nr}, v_{Nr}, which are symbolized by x_1 x_2 x_3 x_4 x_5 x_6, and f_1 and f_2 indicate type 1 and type 2 process faults. We consider two types of process faults, the fault-transformation vectors are

$$\mathbf{f}_1 = [0.1\ \ 0\ \ 2.0\times10^4\ \ 10\ \ 0\ \ 0]^T$$
$$\mathbf{f}_2 = [0\ \ 0\ \ 3.0\times10^4\ \ 10\ \ 0\ \ 0]^T$$

First of all, we obtain the residual model by PCA. The result indicates that the last three eigenvalues are very close to zero and the first three eigenvalues contribute most of the variance of the data set. Thus, in this case, $m = 3$, and the maximal number of zeros is $m - 1 = 2$. In order to isolate 8 different faults (6 sensor faults and 2 process faults), we have to assign at least one zero for this purpose. Thus, we must reserve at most one zero for possible disturbance. Obviously, we are only able to decouple one disturbance. The disturbance direction vector is given by

$$\mathbf{k} = [0.5 \;\; 0 \;\; 2.0{\times}10^4 \;\; 4.0{\times}10^4 \;\; 4.0{\times}10^4 \;\; 10 \;\; 0 \;\; 0]^T$$

We assume three types of sensor faults associated with L, P_2 , v_{Nr}. The fault sizes are roughly 8%, 1.6%, and 1.5% of the respective average in the normal situation. For process faults, we simulate a # 1 process fault, which is a step-likely fault and whose amount is 0.6, and a # 2 fault, which is an x^2-likely fault. All the faults occur at sample 500. At the same time, we add one scalar disturbance in all the simulations. Its size is 0.5.

As for simultaneous fault detection and isolation of sensor and process faults, the situation will be much more complicated than the single fault case. If one ignores sensor problems and tries to detect process faults, this will not work if both sensor fault and process occur. Similarly, if one ignores process faults and tries to detect sensor faults, this will not work if both sensor and process faults occur.

Now we will use some simulations to illustrate the above points. Table 3 shows two structured residual designs. One is for sensor FDI by assuming no process faults and the other one is for process FDI by assuming perfect sensors.

Table 3: Two incidence matrices for sensor and process FDI

Sensor FDI design (assuming no process faults)

	x_1	x_2	x_3	x_4	x_5	x_6
r_1	0	1	1	1	1	1
r_2	1	0	1	1	1	1
r_3	1	1	0	1	1	1
r_4	1	1	1	0	1	1
r_5	1	1	1	1	0	1
r_6	1	1	1	1	1	0

Process FDI design (assuming perfect sensors)

	p_1	p_2
r_1	0	1
r_2	1	0

We consider one case of simultaneous faults: simultaneous #6 sensor fault and #1 process fault. In Fig. 5, we tried to detect and isolate sensor faults by assuming no process faults. It can be seen that all structured residuals went up. Hence we were not able to isolate the sensor faults. In Fig. 5, we also tried to detect and isolate the process faults by assuming perfect sensors. Since all residuals went up, we could not isolate these process faults. In order to detect simultaneous fault, we have to use the unified approach below.
Here we design the structured residual as shown in Table 4. It can be seen that each fault (single or simultaneous) has a unique code or signature.

Table 4: Incidence matrix for simultaneous FDI of sensor and process faults

	x_1	x_2	x_3	x_4	x_5	x_6	f_1	f_2	x_1f_1	x_2f_1	x_3f_1
r_1	0	1	1	1	1	1	0	1	0	1	1
r_2	1	0	1	1	1	1	0	1	1	0	1
r_3	1	1	0	1	1	1	0	1	1	1	0
r_4	1	1	1	0	1	1	0	1	1	1	1
r_5	1	1	1	1	0	1	0	1	1	1	1
r_6	1	1	1	1	1	0	0	1	1	1	1
r_7	0	1	1	1	1	1	1	0	1	1	1
r_8	1	0	1	1	1	1	1	0	1	1	1
r_9	1	1	0	1	1	1	1	0	1	1	1
r_{10}	1	1	1	0	1	1	1	0	1	1	1
r_{11}	1	1	1	1	0	1	1	0	1	1	1
r_{12}	1	1	1	1	1	0	1	0	1	1	1

	x_4f_1	x_5f_1	x_6f_1	x_1f_2	x_2f_2	x_3f_2	x_4f_2	x_5f_2	x_6f_2
r_1	1	1	1	1	1	1	1	1	1
r_2	1	1	1	1	1	1	1	1	1
r_3	1	1	1	1	1	1	1	1	1
r_4	0	1	1	1	1	1	1	1	1
r_5	1	0	1	1	1	1	1	1	1
r_6	1	1	0	1	1	1	1	1	1
r_7	1	1	1	0	1	1	1	1	1
r_8	1	1	1	1	0	1	1	1	1
r_9	1	1	1	1	1	0	1	1	1
r_{10}	1	1	1	1	1	1	0	1	1
r_{11}	1	1	1	1	1	1	1	0	1
r_{12}	1	1	1	1	1	1	1	1	0

Three simulations have been performed: (1) the # 6 sensor fault, (2) the #1 process fault, (3) the simultaneous #6 sensor fault and #1 process fault. The structured residual responses are shown in Figures 6-a, 7-a, 8-a, respectively. The results of fault size identification for them are shown in Figures 6-b, 7-b, 8-b, respectively.

The residual plot in Fig. 6 responds $[1\;\;1\;\;1\;\;1\;\;1\;\;0\;\;1\;\;1\;\;1\;\;1\;\;1\;\;0]^T$ (in the row-counted order) and it indicates the #6 senor fault. The residual plot in Fig.7 gives $[0\;0\;\;0\;\;0\;\;0\;\;0\;\;1\;\;1\;\;1\;\;1\;\;1\;\;1]^T$ and it indicates the # 1 process fault occurs. The residual plot in Fig. 8 gives $[1\;\;1\;\;1\;\;1\;\;1\;\;0\;\;1\;\;1\;\;1\;\;1\;\;1\;\;1]^T$ and it indicates the #6 sensor fault and #1 process fault occurs simultaneously.

4. CONCLUSION

The key objective of this research is to develop a systematic scheme to extract fault features in the presence of sensor faults, process faults, and disturbances. We have successfully developed such a systematic scheme. In particular, we have achieved the following important results:

A tank model that has some common characteristics to a NASA testbed has been developed. The model is nonlinear.

Process fault 1 and sensor fault #6

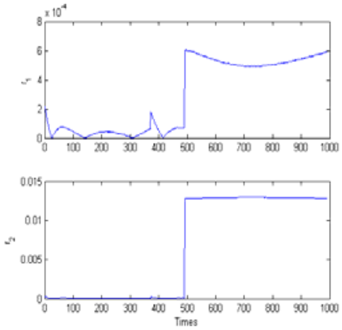

Sensor fault #6 and process fault #1

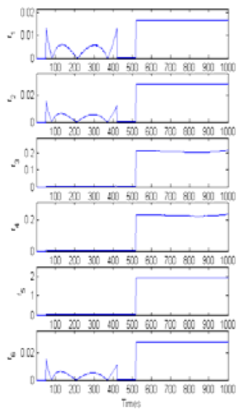

Fig. 5: The performance is not good because we ignore either the process or sensor faults in our design.

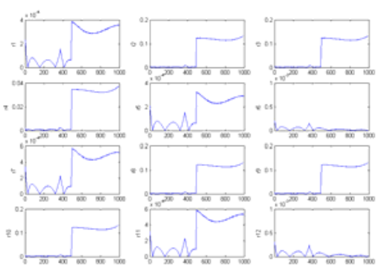

Fig. 6-a: Sensor fault #6

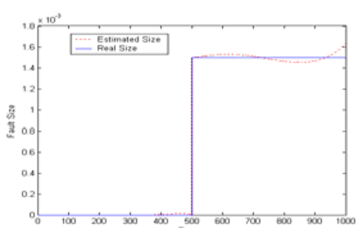

Fig. 6-b: Fault size identification (sensor fault #6)

A systematic FDI algorithm for simultaneous detection and isolation of sensor and process faults has been developed and verified. The algorithm works well even in the presence of unknown process disturbances. Simulations by using the tank system demonstrated the performance of this method.

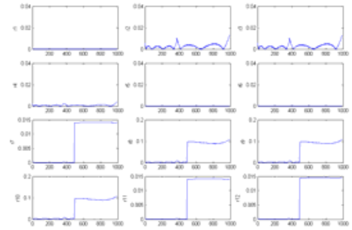

Fig. 7-a: Process fault #1

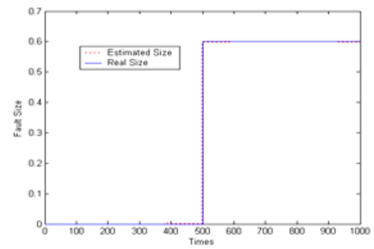

Fig. 7-b: Fault size identification (process fault #1)

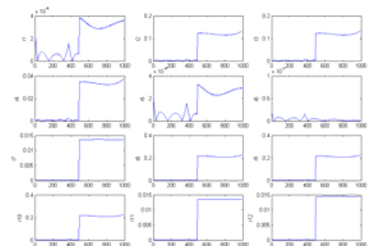

Fig. 8-a: Simultaneous sensor fault #6 and process fault #1

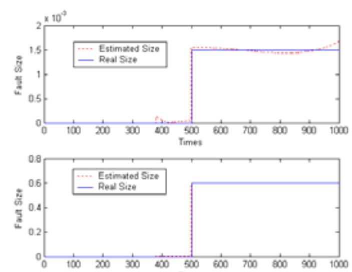

Fig. 8-b: Fault size identification (simul. sensor fault #6 and process fault #1)

REFERENCES

Gerhart, P.M., Gross, R.J., and Hochstein, J.I., (1992) “Fundamentals of Fluid Mechanics, 2nd edition”, *Addison Wesley*, MA,

Marlin, T.E., “Process Control”, (1995), *McGraw-Hill*, New York,

Xu, R. and Kwan, C., (2003) “Robust Isolation of Sensor Failures”, *Asian Journal of Control*.